

# Theoretical predictions for $t\bar{t}W$ cross sections at approximate N<sup>3</sup>LO

---

**Nikolaos Kidonakis\* and Chris Foster**

*Department of Physics, Kennesaw State University,  
Kennesaw, GA 30144, USA*

*E-mail:* [nkidonak@kennesaw.edu](mailto:nkidonak@kennesaw.edu)

We present theoretical calculations of higher-order QCD and electroweak corrections for the associated production of a top-antitop quark pair and a  $W$  boson ( $t\bar{t}W$  production) at LHC energies. We show predictions for cross sections at approximate N<sup>3</sup>LO (aN<sup>3</sup>LO) which include second-order and third-order soft-gluon corrections added to the exact NLO QCD+electroweak result. We compare our results to recent measurements from the LHC, and we find that our predictions provide improved agreement with the data. We also calculate the top-quark transverse momentum and rapidity distributions in  $t\bar{t}W$  production. We find significant enhancements from the higher-order corrections to the total and differential cross sections for this process.

*31st International Workshop on Deep Inelastic Scattering (DIS2024)  
8–12 April 2024  
Grenoble, France*

---

\*Speaker

## 1. Introduction

Measurements of cross sections of  $t\bar{t}W$  events in proton collisions at the LHC are significantly higher than past theoretical predictions. The QCD corrections for  $t\bar{t}W$  production are large and are dominated by soft-gluon emission [1], while the electroweak corrections are smaller. Thus, further improvement in theoretical accuracy can be achieved by the inclusion of higher-order soft-gluon corrections. In this contribution, we present approximate NNLO (aNNLO) and approximate  $N^3LO$  (aN $^3LO$ ) predictions for this process (see Ref. [1] for more details).

## 2. Soft-gluon corrections in $t\bar{t}W$ production

The partonic processes for  $t\bar{t}W$  production are  $q(p_q) + \bar{q}'(p_{\bar{q}'}) \rightarrow t(p_t) + \bar{t}(p_{\bar{t}}) + W(p_W)$ . We define  $s = (p_q + p_{\bar{q}'})^2$ ,  $t = (p_q - p_t)^2$ ,  $u = (p_{\bar{q}'} - p_t)^2$ , and the threshold variable  $s_4 = (p_{\bar{t}} + p_W + p_g)^2 - (p_{\bar{t}} + p_W)^2 = s + t + u - m_t^2 - (p_{\bar{t}} + p_W)^2$  where a gluon with momentum  $p_g$  is emitted. At partonic threshold,  $p_g \rightarrow 0$  and thus  $s_4 \rightarrow 0$ . For the order  $\alpha_s^n$  corrections, the soft-gluon contributions take the form of coefficients multiplying  $[\ln^k(s_4/m_t^2)/s_4]_+$  with  $k \leq 2n - 1$ . We resum these soft corrections for the double-differential cross section in  $p_T$  and rapidity [1, 2].

The factorized hadronic cross section can be written as

$$d\sigma_{pp \rightarrow t\bar{t}W} = \sum_{q, \bar{q}'} \int dx_a dx_b \phi_{q/p}(x_a, \mu_F) \phi_{\bar{q}'/p}(x_b, \mu_F) d\hat{\sigma}_{q\bar{q}' \rightarrow t\bar{t}W}(s_4, \mu_F) \quad (1)$$

where the  $\phi$  denote parton distribution functions (pdf) and  $\hat{\sigma}$  is the partonic cross section.

We take Laplace transforms  $d\tilde{\sigma}_{q\bar{q}' \rightarrow t\bar{t}W}(N) = \int (ds_4/s) e^{-Ns_4/s} d\hat{\sigma}_{q\bar{q}' \rightarrow t\bar{t}W}(s_4)$  and  $\tilde{\phi}(N) = \int_0^1 e^{-N(1-x)} \phi(x) dx$  with transform variable  $N$ . Then, at parton level we have

$$d\tilde{\sigma}_{q\bar{q}' \rightarrow t\bar{t}W}(N) = \tilde{\phi}_{q/q}(N_q, \mu_F) \tilde{\phi}_{\bar{q}'/\bar{q}'}(N_{\bar{q}'}, \mu_F) d\tilde{\sigma}_{q\bar{q}' \rightarrow t\bar{t}W}(N, \mu_F). \quad (2)$$

A refactorization of the cross section is given by

$$d\sigma_{q\bar{q}' \rightarrow t\bar{t}W}(N) = \tilde{\psi}_q(N_q, \mu_F) \tilde{\psi}_{\bar{q}'}(N_{\bar{q}'}, \mu_F) \text{tr} \left\{ H_{q\bar{q}' \rightarrow t\bar{t}W} \tilde{S}_{q\bar{q}' \rightarrow t\bar{t}W} \left( \frac{\sqrt{s}}{N\mu_F} \right) \right\} \quad (3)$$

where  $\psi_q, \psi_{\bar{q}'}$  describe collinear emission from incoming partons,  $H_{q\bar{q}' \rightarrow t\bar{t}W}$  is a short-distance hard function, and  $S_{q\bar{q}' \rightarrow t\bar{t}W}$  is a soft function for noncollinear soft gluons. Thus, from Eq. (2) and (3) we get

$$d\tilde{\sigma}_{q\bar{q}' \rightarrow t\bar{t}W}(N) = \frac{\tilde{\psi}_{q/q}(N_q, \mu_F) \tilde{\psi}_{\bar{q}'/\bar{q}'}(N_{\bar{q}'}, \mu_F)}{\tilde{\phi}_{q/q}(N_q, \mu_F) \tilde{\phi}_{\bar{q}'/\bar{q}'}(N_{\bar{q}'}, \mu_F)} \text{tr} \left\{ H_{q\bar{q}' \rightarrow t\bar{t}W} \tilde{S}_{q\bar{q}' \rightarrow t\bar{t}W} \left( \frac{\sqrt{s}}{N\mu_F} \right) \right\}. \quad (4)$$

The soft function  $S_{q\bar{q}' \rightarrow t\bar{t}W}$  satisfies the renormalization group equation

$$\left( \mu_R \frac{\partial}{\partial \mu_R} + \beta(g_s) \frac{\partial}{\partial g_s} \right) S_{q\bar{q}' \rightarrow t\bar{t}W} = -\Gamma_{S_{q\bar{q}' \rightarrow t\bar{t}W}}^\dagger S_{q\bar{q}' \rightarrow t\bar{t}W} - S_{q\bar{q}' \rightarrow t\bar{t}W} \Gamma_{S_{q\bar{q}' \rightarrow t\bar{t}W}}. \quad (5)$$

The soft anomalous dimension  $\Gamma_{S_{q\bar{q}' \rightarrow t\bar{t}W}}$  controls the evolution of the soft function which gives the exponentiation of logarithms of  $N$  [1–3]. Renormalization group evolution leads to resummation.

We choose a color tensor basis of  $s$ -channel singlet and octet exchange  $c_1^{q\bar{q}'\rightarrow t\bar{t}W} = \delta_{ab}\delta_{12}$ ,  $c_2^{q\bar{q}'\rightarrow t\bar{t}W} = T_{ba}^c T_{12}^c$ . The four matrix elements of  $\Gamma_S^{q\bar{q}'\rightarrow t\bar{t}W}$  are at one loop

$$\begin{aligned}\Gamma_{11}^{(1)}{}_{q\bar{q}'\rightarrow t\bar{t}W} &= \Gamma_{\text{cusp}}^{(1)}, & \Gamma_{12}^{(1)}{}_{q\bar{q}'\rightarrow t\bar{t}W} &= \frac{C_F}{2N_c} \Gamma_{21}^{(1)}{}_{q\bar{q}'\rightarrow t\bar{t}W}, & \Gamma_{21}^{(1)}{}_{q\bar{q}'\rightarrow t\bar{t}W} &= \ln\left(\frac{t_1 t'_1}{u_1 u'_1}\right), \\ \Gamma_{22}^{(1)}{}_{q\bar{q}'\rightarrow t\bar{t}W} &= \left(1 - \frac{C_A}{2C_F}\right) \left[ \Gamma_{\text{cusp}}^{(1)} + 2C_F \ln\left(\frac{t_1 t'_1}{u_1 u'_1}\right) \right] + \frac{C_A}{2} \left[ \ln\left(\frac{t_1 t'_1}{s m_t^2}\right) - 1 \right],\end{aligned}$$

where  $\Gamma_{\text{cusp}}^{(1)} = -C_F (L_{\beta_t} + 1)$  is the one-loop QCD massive cusp anomalous dimension, with  $L_{\beta_t} = (1 + \beta_t^2)/(2\beta_t) \ln[(1 - \beta_t)/(1 + \beta_t)]$  and  $\beta_t = \sqrt{1 - 4m_t^2/s'}$ ,  $s' = (p_t + p_{\bar{t}})^2$ ,  $t_1 = t - m_t^2$ ,  $u_1 = u - m_t^2$ ,  $t'_1 = (p_{\bar{q}'} - p_{\bar{t}})^2 - m_t^2$ ,  $u'_1 = (p_q - p_{\bar{t}})^2 - m_t^2$ .

At two loops, we find

$$\begin{aligned}\Gamma_{11}^{(2)}{}_{q\bar{q}'\rightarrow t\bar{t}W} &= \Gamma_{\text{cusp}}^{(2)}, \\ \Gamma_{12}^{(2)}{}_{q\bar{q}'\rightarrow t\bar{t}W} &= \left(K_2 - C_A N_2^{\beta_t}\right) \Gamma_{12}^{(1)}{}_{q\bar{q}'\rightarrow t\bar{t}W}, & \Gamma_{21}^{(2)}{}_{q\bar{q}'\rightarrow t\bar{t}W} &= \left(K_2 + C_A N_2^{\beta_t}\right) \Gamma_{21}^{(1)}{}_{q\bar{q}'\rightarrow t\bar{t}W}, \\ \Gamma_{22}^{(2)}{}_{q\bar{q}'\rightarrow t\bar{t}W} &= K_2 \Gamma_{22}^{(1)}{}_{q\bar{q}'\rightarrow t\bar{t}W} + \left(1 - \frac{C_A}{2C_F}\right) \left( \Gamma_{\text{cusp}}^{(2)} - K_2 \Gamma_{\text{cusp}}^{(1)} \right) + \frac{1}{4} C_A^2 (1 - \zeta_3),\end{aligned}$$

where  $\Gamma_{\text{cusp}}^{(2)}$  is the two-loop massive cusp anomalous dimension in QCD [4] and  $N_2^{\beta_t}$  is given in [1].

### 3. $t\bar{t}W$ cross section

We employ fixed-order expansions of the resummed cross section so that no prescription is needed or used, and this avoids underestimating the size of the corrections (further references and a discussion of the differences to work that uses other formalisms and kinematics can be found in [1]). The NLO expansions closely approximate exact NLO results for total cross sections and top-quark  $p_T$  and rapidity distributions. The NNLO expansions (aNNLO) are consistent with (partially exact) NNLO results for total cross sections [5]. The aN<sup>3</sup>LO calculation provides the state of the art, and electroweak corrections are also included.

The left plot in Fig. 1 shows the aN<sup>3</sup>LO QCD+NLO EW  $t\bar{t}W$  cross section versus LHC energy. In addition to the central result (with  $\mu = m_t = 172.5$  GeV using MSHT20 NNLO pdf [6]), the variations from scale and scale+pdf uncertainties are also shown. ATLAS and CMS data at 8 TeV [7, 8] and 13 TeV [9, 10] are also shown, and we find improved agreement. The plot on the right in Fig. 1 shows the results at each perturbative order from LO QCD all the way to aN<sup>3</sup>LO QCD+NLO EW. The  $K$ -factors over LO QCD are large and are displayed in the inset plot.

At 13.6 TeV, the NLO QCD corrections provide a 47% enhancement, the aNNLO QCD corrections an additional 17%, the aN<sup>3</sup>LO QCD corrections another 6%, and the electroweak NLO corrections around 7%. The total aN<sup>3</sup>LO QCD+NLO EW cross section is 78% bigger than the LO QCD result. We note that the  $t\bar{t}W^+$  cross sections are larger than those for  $t\bar{t}W^-$  but the corrections are slightly bigger for  $t\bar{t}W^-$ .

We proceed with a comparison with 8 and 13 TeV CMS and ATLAS data. The NLO and even aNNLO results are not sufficient, and we need aN<sup>3</sup>LO corrections to describe the data. At 8 TeV,

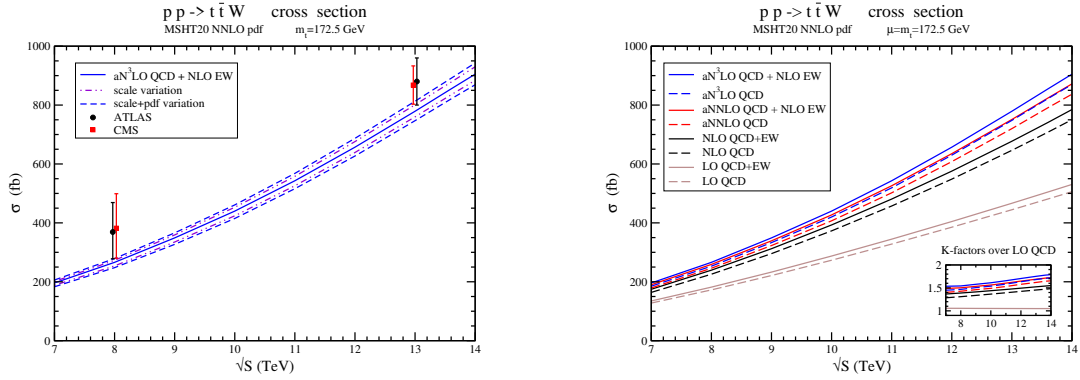


**Figure 1:**  $t\bar{t}W$  production cross sections at LHC energies.

the measurement from ATLAS is  $369^{+100}_{-91}$  fb [7], and from CMS it is  $382^{+117}_{-102}$  fb [8]. The theoretical prediction at  $aN^3LO$  QCD + NLO EW is  $266^{+7}_{-12} +6_{-6}$  fb.

At 13 TeV, CMS finds  $868 \pm 65$  fb with  $t\bar{t}W^+$   $553 \pm 42$  fb and  $t\bar{t}W^-$   $343 \pm 36$  fb [9] while ATLAS finds  $880 \pm 80$  fb with  $t\bar{t}W^+$   $583 \pm 58$  fb and  $t\bar{t}W^-$   $296 \pm 40$  fb [10]. The theoretical prediction at  $aN^3LO$  QCD + NLO EW is  $779^{+22}_{-19} +12_{-13}$  fb with  $t\bar{t}W^+$   $517^{+14}_{-12} +8_{-9}$  fb and  $t\bar{t}W^-$   $262^{+8}_{-7} +4_{-4}$  fb.

#### 4. Top-quark differential distributions in $t\bar{t}W$ production

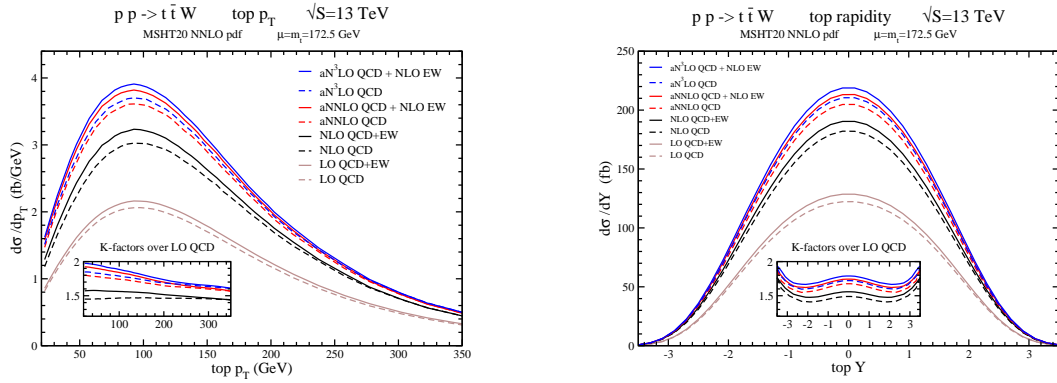


**Figure 2:** Top-quark  $p_T$  (left) and rapidity (right) distributions in  $t\bar{t}W$  production at 13 TeV energy.

In Fig. 2, we display on the left plot the top-quark transverse-momentum ( $p_T$ ) distribution in  $t\bar{t}W$  production for various orders from LO QCD through  $aN^3LO$  QCD+NLO EW at 13 TeV energy. The inset plot shows the  $K$ -factors, which decrease at larger top  $p_T$ . The plot on the right shows the corresponding results for the top-quark rapidity distribution. As seen from the inset plot, the  $K$ -factors increase at larger rapidities.

## 5. Conclusion

We have presented results through a  $N^3LO$  QCD+NLO EW for  $t\bar{t}W$  production, including cross sections and top-quark  $p_T$  and rapidity distributions. The soft-gluon corrections are dominant, they are large, and they improve agreement with data from the LHC.

## Acknowledgments

This material is based upon work supported by the National Science Foundation under Grant No. PHY 2112025.

## References

- [1] N. Kidonakis and C. Foster, *Soft-gluon corrections in  $t\bar{t}W$  production*, *Phys. Lett. B* **854**, 138708 (2024) [arXiv:2312.00861].
- [2] M. Forslund and N. Kidonakis, *Resummation for  $2 \rightarrow n$  processes in single-particle-inclusive kinematics*, *Phys. Rev. D* **102**, 034006 (2020) [arXiv:2003.09021].
- [3] N. Kidonakis, *Next-to-next-to-leading soft-gluon corrections for the top quark cross section and transverse momentum distribution*, *Phys. Rev. D* **82**, 114030 (2010) [arXiv:1009.4935].
- [4] N. Kidonakis, *Two-loop soft anomalous dimensions and next-to-next-to-leading-logarithm resummation for heavy quark production*, *Phys. Rev. Lett.* **102**, 232003 (2009) [arXiv:0903.2561].
- [5] L. Buonocore, S. Devoto, M. Grazzini, S. Kallweit, J. Mazzitelli, L. Rottoli, and C. Savoini, *Precise predictions for the associated production of a  $W$  boson with a top-antitop quark pair at the LHC*, *Phys. Rev. Lett.* **131**, 231901 (2023) [arXiv:2306.16311].
- [6] S. Bailey, T. Cridge, L.A. Harland-Lang, A.D. Martin, and R.S. Thorne, *Parton distributions from LHC, HERA, Tevatron and fixed target data: MSHT20 PDFs*, *Eur. Phys. J. C* **81**, 341 (2021) [arXiv:2012.04684].
- [7] ATLAS Collaboration, *Measurement of the  $t\bar{t}W$  and  $t\bar{t}Z$  production cross sections in  $pp$  collisions at  $\sqrt{s} = 8$  TeV with the ATLAS detector*, *JHEP* **11**, 172 (2015) [arXiv:1509.05276].
- [8] CMS Collaboration, *Observation of top quark pairs produced in association with a vector boson in  $pp$  collisions at  $\sqrt{s} = 8$  TeV*, *JHEP* **01**, 096 (2016) [arXiv:1510.01131].
- [9] CMS Collaboration, *Measurement of the cross section of top quark-antiquark pair production in association with a  $W$  boson in proton-proton collisions at  $\sqrt{s} = 13$  TeV*, *JHEP* **07**, 219 (2023) [arXiv:2208.06485].
- [10] ATLAS Collaboration, *Measurement of the total and differential cross-sections of  $t\bar{t}W$  production in  $pp$  collisions at  $\sqrt{s} = 13$  TeV with the ATLAS detector*, *JHEP* **05**, 131 (2024) [arXiv:2401.05299].